

Dalton Transactions

Accepted Manuscript



This is an *Accepted Manuscript*, which has been through the Royal Society of Chemistry peer review process and has been accepted for publication.

Accepted Manuscripts are published online shortly after acceptance, before technical editing, formatting and proof reading. Using this free service, authors can make their results available to the community, in citable form, before we publish the edited article. We will replace this *Accepted Manuscript* with the edited and formatted *Advance Article* as soon as it is available.

You can find more information about *Accepted Manuscripts* in the [Information for Authors](#).

Please note that technical editing may introduce minor changes to the text and/or graphics, which may alter content. The journal's standard [Terms & Conditions](#) and the [Ethical guidelines](#) still apply. In no event shall the Royal Society of Chemistry be held responsible for any errors or omissions in this *Accepted Manuscript* or any consequences arising from the use of any information it contains.

Cite this: DOI: 10.1039/c0xx00000x

www.rsc.org/xxxxxx

ARTICLE TYPE

[Dy(acac)₃(dppn)]·C₂H₅OH: Construction of single-ion magnet based on the square-antiprism dysprosium(III) ion

Gong-Jun Chen,^a Yang Zhou,^a Guo-Xia Jin,^a Yu-Bin Dong*^a

Received (in XXX, XXX) Xth XXXXXXXXX 20XX, Accepted Xth XXXXXXXXX 20XX

DOI: 10.1039/b000000x

The present work reports a new mononuclear Dy(III) complex [Dy(acac)₃(dppn)]·C₂H₅OH (**1**) (acac = acetylacetonate, dppn = benzo[*i*]dipyrido-[3, 2-*a*:2', 3'-*c*]phenazine). X-ray crystallography analysis reveals that compound **1** is a discrete molecular complex and the Dy(III) center lies in a square-antiprism coordination environment. Furthermore, complex **1** shows single-ion magnet (SIM) behavior. Compared to the reported complexes [Dy(dppz)(acac)₃]·CH₃OH, [Dy(dpq)(acac)₃] and [Dy(phen)(acac)₃], complex **1** exhibits the different energy barrier, which might be raised from the different coordination environment caused by the different auxiliary co-ligand dppn. The energy barrier variations of these Dy(III)-complexes are consistent with their square antiprism structural features.

Introduction

Single-molecule magnets (SMMs) have attracted much attention in recent years due to their various potential applications such as high-density magnetic memories, magnetic refrigeration, molecular spintronics and as quantum computing devices.¹⁻⁶ A basic requirement for SMMs is the presence of a large total spin angular moment in a single molecule.⁷⁻¹⁰ The origin of the SMMs behavior is the easy axis magnetic anisotropy ($D < 0$), which causes the formation of an energy barrier that prevents reversal of the molecular magnetization, consequently, a slow relaxation of the magnetization at low temperature.¹¹⁻¹³ Besides large ground state, the enhancement of energy barrier and blocking temperature of SMMs is also very important for controlling the magnetic anisotropy.¹⁴⁻¹⁸ Lanthanide ions, especially dysprosium (III), are attractive candidates for the preparation of new single molecule magnets.¹⁹⁻³⁸ The dysprosium(III) ion, possessing a Kramers ground state of 6H_{15/2}, has a large angular moment and is assumed to have a large Ising-type magnetic anisotropy. So dysprosium(III) ion with a suitable coordination environment might be an appealing paramagnetic source for the construction of SMM.³⁹⁻⁴⁵ Owing to the single-ion features, mononuclear Dy(III) SMMs are referred as "Single-Ion Magnets (SIMs)". Up to date, numerous Ln-SIMs are reported, including Ln-phthalocyanine,⁴⁶⁻⁵⁵ Ln-β-diketone⁵⁶⁻⁶² even organometallic lanthanide systems.⁶³⁻⁶⁵ The local symmetry in the reported Ln-SIMs is all defined by a high-order single axis.

So far, the study on the relationship between SMMs and their corresponding metal coordination environments, however, is relatively rare. In addition, a complete and detailed theoretical picture of the relaxation dynamics of the magnetization in lanthanide-SIMs is still immature.⁶⁶ Recently, we observed distinct tunneling rate of the β-diketone-based Dy(III)-SIMs which possess the different auxiliary ligands.⁵⁸⁻⁵⁹ The results indicate that the relaxation rates are extremely sensitive to tiny distortions of the local coordination geometry. Fortunately, the β-diketone-based Ln(III)-coordination spheres can be easily

modified by incorporation of the different auxiliary ligands, which could be a promising approach to probe the dynamics of magnetization.

For more insight into the influence of the auxiliary ligands on the SMMs, in this contribution, the dppn ligand is chosen to be an auxiliary ligand to prepare a new β-diketone-based Dy(III)-SIM [Dy(acac)₃(dppn)]·C₂H₅OH (**1**). Single-crystal structure indicates that the Dy(III) ion in **1** adopts a square-antiprism coordination geometry and exhibits SIM behaviors. Interestingly, complex **1** has the effective energy barrier (37.22 K), while its reported analogues of [Dy(dppz)(acac)₃]·CH₃OH, [Dy(dpq)(acac)₃] and [Dy(phen)(acac)₃] with the same square antiprism geometry, however, show different energy barriers.

Experiment section

Materials and measurements

The reagents and solvents employed were commercially available and used without further purification. Elemental analyses for C, H and N were obtained on a Perkin-Elmer analyzer model 240. The XRD patterns were collected by a D8 ADVANCE X-ray powder diffractometer (XRD) with Cu Kα radiation ($\lambda = 1.5405 \text{ \AA}$). All magnetization data were recorded on a Quantum Design MPMS-XL7 SQUID magnetometer. The variable-temperature magnetization was measured with an external magnetic field of 1000 Oe in the temperature range of 1.9-300 K. The diamagnetic corrections for the compounds were estimated using Pascal's constants, and magnetic data were corrected for diamagnetic contributions of the sample holder.

Synthesis of [Dy(acac)₃(dppn)]·C₂H₅OH (**1**)

To a solution of acetylacetonate (0.11 mL, 1.0 mmol) and Et₃N (0.14 mL, 0.10 mmol) in MeOH/EtOH (1:1 v/v, 20 mL), Dy(NO₃)₃·6H₂O (0.114 g, 0.25 mmol) was added. The solution was stirred for 15 min followed by addition of the diimine base dppn (0.083 g, 0.25 mmol). The mixture was refluxed for 3 h in air and then filtered. Red block crystals suitable for single-crystal X-ray diffraction were obtained by slow evaporation of the filtrate after several weeks. Yield: 35% (based on the Dy(III)

salt). Anal. Calcd. for $C_{39}H_{38}DyN_4O_7$: C, 55.45; H, 4.57; N, 6.69. Found: C, 55.40; H, 4.60; N, 6.71.

X-ray crystallography

Diffraction data for the complex was collected at 293 (2) K, with a Bruker Smart 1000 CCD diffractometer using Mo-K α radiation ($\lambda = 0.71073 \text{ \AA}$) with the ω -2 θ scan technique. An empirical absorption correction was applied to raw intensities.⁶⁷ The structure was solved by direct methods (SHELX-97) and refined with full-matrix least-squares technique on F² using the SHELX-97.⁶⁸ The hydrogen atoms were added theoretically, and riding on the concerned atoms and refined with fixed thermal factors. The details of crystallographic data and structure refinement parameters are summarized in Table 1. The crystallographic data in CIF format and check CIF for complex **1** are available in Supporting Information, and the structural analysis have been deposited with the Cambridge Crystallographic Data Centre with CCDC: 1007462.

Table 1 Data collection and processing parameters for complex **1**

Complex	1
Empirical formula	$C_{39}H_{38}DyN_4O_7$
Formula weight	837.23
Crystal system,	Monoclinic
space group	P-1
$a / \text{\AA}$	10.4228(12)
$b / \text{\AA}$	12.4496(14)
$c / \text{\AA}$	14.2131(10)
$\alpha / ^\circ$	103.621(8)
$\beta / ^\circ$	93.468(8)
$\gamma / ^\circ$	96.219(9)
$V / \text{\AA}^3$	1774.8(3)
Z	2
Density (calc.) / $\text{mg}\cdot\text{m}^{-3}$	1.567
μ / mm^{-1}	2.161
F(000)	844
Wavelength / \AA	0.71073 \AA
θ range for data collection / $^\circ$	2.36 to 29.39 deg
Reflections collected / unique	13956/9786
Data / restraints / parameters	8101/0/467
Goodness-of-fit on F^2	1.040
R_1 / wR_2	$R_1 = 0.0480, wR_2 = 0.0860$
Largest diff. peak / $e\cdot\text{\AA}^{-3}$	1.834 and -1.156

Results and discussion

Crystal structure of **1**

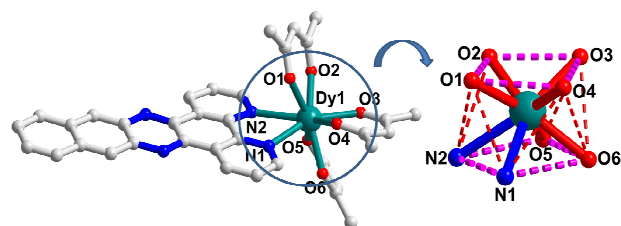


Fig. 1 Molecular structure of **1**.

Compound **1** was isolated as a molecular complex which was confirmed by single-crystal X-ray crystallography. The selected bond lengths and angles are given in Table 2. Complex **1** crystallizes in the monoclinic space group P-1. As shown in Fig.

1, Dy(III) center lies in a square anti-prism eight-coordinated sphere which is defined by six O-donors from three deprotonated β -diketonate ligands and two N-donors from a bidentate dppn ligand. The Dy-O bond distances range from 2.305-2.354 \AA . One square base of the square antiprism is formed by the four oxygen atoms (O1, O2, O3 and O4) from two chelating β -diketonate ligands, and the other one is constructed by two oxygen (O5 and O6) and two nitrogen donors (N1 and N2) from one β -diketonate and one dppn chelating ligands, respectively. A square antiprism can be described by two crucial parameters; that is Φ (skew angle) and α (the angle between the S8 axis and a RE-L direction). The corresponding numerical values of Φ and α for a regular square antiprism (SAP) are 45° and 54.74° , respectively.⁶⁶ The S8 axis define is the line of Dy with the center of one square base of the square antiprism.

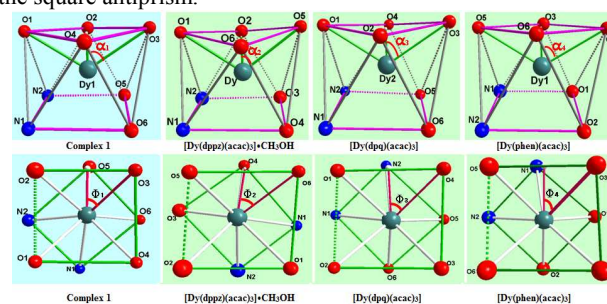


Fig. 2 Comparison of Φ and α between complex **1**, and its $[\text{Dy}(\text{dppz})(\text{acac})_3]\cdot\text{CH}_3\text{OH}$, $[\text{Dy}(\text{dpq})(\text{acac})_3]$ and $[\text{Dy}(\text{phen})(\text{acac})_3]$ analogues.

Table 2 Selected bonds lengths and angles for **1**.

1	Dy(1)-O(1)	2.354(3)	Dy(1)-O(2)	2.305(3)
	Dy(1)-O(3)	2.314(3)	Dy(1)-O(4)	2.327(3)
	Dy(1)-O(5)	2.347(3)	Dy(1)-O(6)	2.321(3)
	Dy(1)-N(1)	2.561(4)	Dy(1)-N(2)	2.604(4)
	O(2)-Dy(1)-O(1)	73.55(10)	O(3)-Dy(1)-O(1)	114.63(11)
	O(3)-Dy(1)-O(6)	83.33(12)	O(2)-Dy(1)-O(4)	119.85(11)
	O(3)-Dy(1)-O(5)	80.14(11)	O(4)-Dy(1)-O(5)	140.73(12)
	O(2)-Dy(1)-N(1)	134.46(12)	O(6)-Dy(1)-N(1)	73.53(12)
	O(6)-Dy(1)-N(2)	111.17(11)	N(1)-Dy(1)-N(2)	62.74(12)

Recently, similar mononuclear complexes $[\text{Dy}(\text{dppz})(\text{acac})_3]\cdot\text{CH}_3\text{OH}$, $[\text{Dy}(\text{dpq})(\text{acac})_3]$ and $[\text{Dy}(\text{phen})(\text{acac})_3]$ were reported by us. Based on the analysis of their Φ , α and bond lengths (Fig. 2, Fig. S1 and Table 3), the Dy-square antiprism coordination sphere could be modified by changing the auxiliary ligands. For example, compared to the standard skew angle of 45° for the square antiprism, the angle deviation in **1**, $[\text{Dy}(\text{dppz})(\text{acac})_3]\cdot\text{CH}_3\text{OH}$, $[\text{Dy}(\text{dpq})(\text{acac})_3]$ and $[\text{Dy}(\text{phen})(\text{acac})_3]$ is respectively 3.10° , 0.77° , 1.98° and 2.42° , which is resulted from the different auxiliary ligands. As indicated in Fig. 2, $[\text{Dy}(\text{dppz})(\text{acac})_3]\cdot\text{CH}_3\text{OH}$ represents the best fit to the idealized square antiprism, while compound **1** exhibits the most distorted square antiprism.

Table 3 Compare to the bonds lengths (\AA) and angles (deg) for **1**, $[\text{Dy}(\text{dppz})(\text{acac})_3]\cdot\text{CH}_3\text{OH}$ (**2**), $[\text{Dy}(\text{dpq})(\text{acac})_3]$ (**3**) and $[\text{Dy}(\text{phen})(\text{acac})_3]$ (**4**).

1	O(1)-O(2)	2.790(4)	O(2)-O(3)	2.804(5)
	O(3)-O(4)	2.804(4)	O(4)-O(1)	2.837(5)
	$\alpha 1$	57.84°	$\Phi 1$	55.39(8)°
	α_{average}	58.63°	Φ_{average}	56.82°
	Dy...Dy (The shortest distance)	7.407 Å		
2	O(1)-O(2)	2.775(15)	O(2)-O(5)	2.736(18)
	O(5)-O(6)	2.777(16)	O(6)-O(1)	2.788(17)
	$\alpha 2$	55.51°	$\Phi 2$	44.89(31)°
	α_{average}	57.41°	Φ_{average}	56.71°
	Dy...Dy (the shortest distance)	7.34 Å		
3	O(1)-O(2)	2.771(12)	O(2)-O(3)	2.831(12)
	O(3)-O(4)	2.786(13)	O(4)-O(1)	2.862(12)
	$\alpha 3$	52.76°	$\Phi 3$	49.89(20)°
	α_{average}	57.93°	Φ_{average}	57.23°
	Dy...Dy (the shortest distance)	8.83 Å		
4	O(3)-O(4)	2.783(6)	O(4)-O(6)	2.925(4)
	O(6)-O(5)	2.762(6)	O(5)-O(3)	2.830(4)
	$\alpha 4$	57.16°	$\Phi 4$	51.46(9)°
	α_{average}	58.15°	Φ_{average}	57.38°
	Dy...Dy (the shortest distance)	8.243 Å		

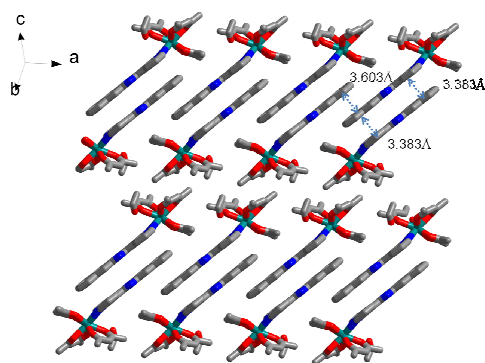


Fig. 3 Packing arrangement of **1**.

The crystal packing reveals that the one-dimensional (1D) supramolecular tapes driven by the intermolecular π - π stacking exist in **1**. As indicated in Fig. 3, the dppn ligands attached to Dy(III) centers stack one on top of another in a parallel fashion leading to a head to tail arrangement. The centroid-to-centroid distances between the corresponding intermolecular aromatic rings are 3.383 and 3.603 Å, respectively. The shortest Dy...Dy distance in **1** is 7.407 Å (Fig. S2, ESI), which is slightly longer than that of in [Dy(dppz)(acac)₃]-CH₃OH (7.34 Å), but significantly shorter than those of in [Dy(dppz)(acac)₃]-CH₃OH (8.83 Å) and [Dy(dpq)(acac)₃] (8.243 Å). The measured XRPD pattern of **1** (Fig. S3, ESI) is well in correspondence with that of simulated one, indicating that the bulk sample of **1** was obtained in pure phase.

Magnetic property

Direct-current (dc) magnetic susceptibility of **1** has been measured in an applied magnetic field of 0.1 T between 300 and 1.9 K. At room temperature (300 K), the $\chi_m T$ value is 14.20 cm³ K mol⁻¹ (Fig. 4) which is close to the expected value of 14.18 cm³ K mol⁻¹ for a Dy(III) unit ($S = 5/2$, $L = 5$, $g = 4/3$, $6H_{15/2}$, $C = 14.18$ cm³ K mol⁻¹).⁶⁹ The $\chi_m T$ value gradually decreases with the temperature decreasing in the range of 300-110K. The sharp decrease below 110K was observed which might be ascribed to the progressive depopulation of excited Stark sublevels of Dy(III)

and/or the very weak intermolecular magnetic interactions between Dy(III) ions.⁷⁰

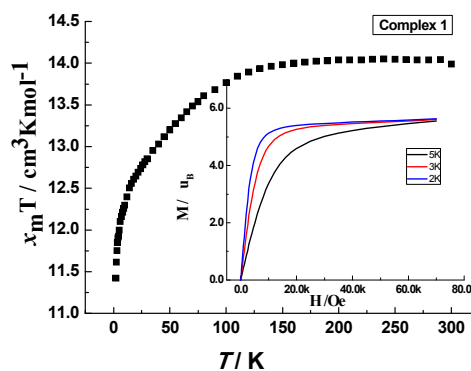


Fig. 4 Temperature dependence of the $\chi_m T$ values at 1 kOe for **1**. Inset: M vs. H/T plot at different temperatures for **1**.

To investigate the dynamics of the magnetization, magnetization relaxation data of **1** were collected at varied temperature while the frequencies of the microcrystalline were held constant. At a fixed frequency, the in-phase (χ') and the out-of-phase (χ'') components of the ac magnetic susceptibility were measured as the frequencies (ν) of the ac field varied from 1.9 K to 22 K. Compound **1** shows the frequency dependencies of the alternating current (ac) susceptibilities under zero-dc field, which reveals the typical features associated with the SIMs behavior (Fig. 5). The maximum magnetization at 1.9 K is 5.85 μ_B , which is lower than the expected saturation value of 10 μ_B for each Dy(III) ion. From the M vs. H/T data measured in different magnetic fields (inset Fig. 4) of **1** show non-superposition, suggesting the presence of a significant magnetic anisotropy and/or low lying excited states. Eight-coordination mode of compound **1** made Dy(III) ion splitting of the $J = 15/2$, which effects the magnetic anisotropy strongly and display a SMM behavior.⁷¹

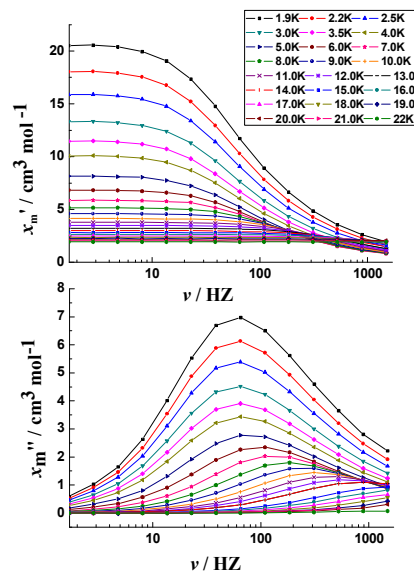


Fig. 5 Frequency dependence of the in-phase χ' (top) and out-of-phase χ'' (bottom) components of the alternating-current (ac) susceptibility for compound **1** measured under zero static field in

the temperature range of 1.9–22 K.

Cole–Cole diagrams (Fig. 6) in the form of χ' vs. χ'' with nearly semi-circle shape have also been obtained. These data have been fitted to the generalized Debye model,^{72–73}

$$\chi_{(\nu)} = \chi_S + \frac{\chi_T - \chi_S}{1 + (i\nu\tau)^{1-\alpha}}$$

where χ_T is the isothermal susceptibility, χ_S is the adiabatic susceptibility, ν is the frequency of the ac field, and τ is the relaxation time of the system. The Cole–Cole plots of compound **1** affords α values which increase to 0.210 (1.9 K) at the lowest temperature and decrease to 0.131 (9 K) at high temperature (Fig. S4). The result indicates that a single relaxation time is mainly involved in the present relaxation process.⁷⁴ The α value is in the range of previously reported SMMs and SCMs,^{40–42} which excludes the possibility of spin-glass.

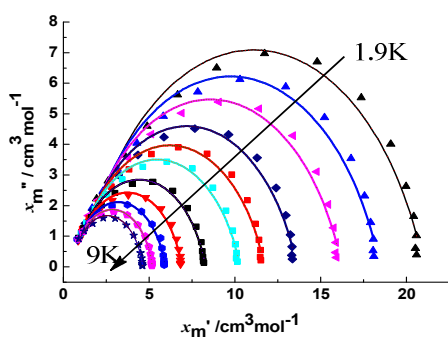


Fig. 6 The Cole–Cole plots at 1.9–9 K of **1** in zero-dc field. The solid lines are the best fit to the experimental data.

In addition, the observed peaks of the out-of-phase signals correspond to the coincidence of the applied ac field oscillation frequency with the relaxation rate. Compound **1** at a selected frequency goes through a maximum and the maximum shift to high temperature with increasing frequency, which is the nature of super paramagnet. Data obtained with varying frequencies of oscillation of the ac field are fitted with Arrhenius law.⁷⁵ We can derive the magnetization relaxation time in the form of $\ln\tau$ plotted as a function of $1/T$ between 1.9 and 14 K (Fig. 7). Above 9 K the relaxation follows a thermally activated mechanism affording an energy barrier of 37.22 K with a pre-exponential factor (τ_0) of $\tau_0 = 6.72 \times 10^{-7}$ s based on the Arrhenius law [$\tau = \tau_0 \exp(U_{\text{eff}}/kBT)$], where T is the temperature of the maximum χ'' at different frequencies and $\tau = 1/(2\pi\nu)$ (ν is the frequency), which is consistent with the expected τ_0 of 10^{-6} – 10^{-11} for a SMMs.⁶⁰ Relaxation time of complex $[\text{Dy}(\text{dppz})(\text{acac})_3] \cdot \text{CH}_3\text{OH}$ above 8 K shows an energy barrier 187 K, while $[\text{Dy}(\text{dpq})(\text{acac})_3]$ and $[\text{Dy}(\text{phen})(\text{acac})_3]$ have an energy barrier 136 K and 64 K. The different energy barrier for compound **1**, $[\text{Dy}(\text{dppz})(\text{acac})_3] \cdot \text{CH}_3\text{OH}$, $[\text{Dy}(\text{dpq})(\text{acac})_3]$ and $[\text{Dy}(\text{phen})(\text{acac})_3]$ are attributed to the influence of ligand field by auxiliary ligand. On the other hand, it provides the valuable information for the improvement of the SMMs behavior by the perturbation of the auxiliary ligand. Indeed, the Dy...Dy distance would influence the magnetic interactions. As mentioned above,

compound **1** has the shortest Dy...Dy distance but small energy barrier, which indicates the Dy...Dy bond distance has little influence on the magnetic interaction. The magnetic coupling between neighbor lanthanide ions herein should be inappreciably weak due to the large Dy...Dy separation (~ 8 Å). As discussed by Dante Gatteschi, α , the deviation from 54.74° stands for the compression/elongation of SAP along the C4 axis, which might affect the energy difference between the two lowest lying states even if the changes of ground states do not occur, a variation of angle Φ is an important perturbation for Hamiltonian due to the change of symmetry, where the transverse anisotropy is introduced, then promoting the quantum tunneling of the magnetization in these systems.⁵⁷ Here, by changing the auxiliary ligands, the square antiprism is slightly distorted, leading to a longitudinal contraction of the square-antiprism coordination polyhedron (the increase of α). The longitudinal contraction strengthens the interaction between the single lanthanide ion electron density and the crystal field environment, which increase the splitting between the lowest and the second lowest sublevels. The difference in the magnetic anisotropies of **1**, $[\text{Dy}(\text{dppz})(\text{acac})_3] \cdot \text{CH}_3\text{OH}$, $[\text{Dy}(\text{dpq})(\text{acac})_3]$ and $[\text{Dy}(\text{phen})(\text{acac})_3]$ is attributed to the slightly different morphology of the ligand field originating from a slightly different ligands around the Dy(III) ions. Moreover, the energy barriers of **1**, $[\text{Dy}(\text{dppz})(\text{acac})_3] \cdot \text{CH}_3\text{OH}$, $[\text{Dy}(\text{dpq})(\text{acac})_3]$ and $[\text{Dy}(\text{phen})(\text{acac})_3]$ are proportional to the value of the square antiprism. For a regular square antiprism, the RE-L distances are equal, the gap of the longest bond length and the shortest bond length are 0.299(**1**), 0.273($[\text{Dy}(\text{dppz})(\text{acac})_3] \cdot \text{CH}_3\text{OH}$), 0.278($[\text{Dy}(\text{dpq})(\text{acac})_3]$) and 0.280 ($[\text{Dy}(\text{phen})(\text{acac})_3]$), respectively. The gap of the bonds lengths are also proportional to the value of the square antiprism. The shortest Dy...Dy distance in **1** is 7.407 Å, which should weaken the intermetallic magnetic coupling and the influence of the intermolecular interactions can be ignored. The slow magnetization relaxation should be assigned to SIM behavior.

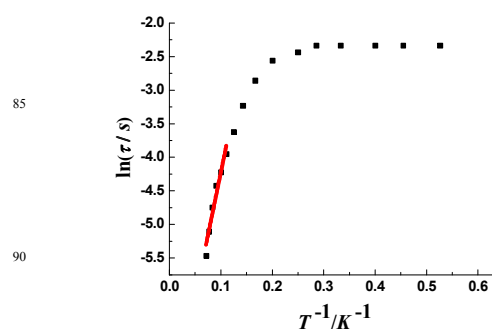


Fig. 7 Magnetization relaxation time, $\ln\tau$ vs. T^{-1} plot for **1** under zero-dc field. The red line is fitted with the Arrhenius law.

The field dependence of the magnetization of **1** was also measured at 1.9 K to check for hysteresis, i.e., slow relaxation of the magnetization. The M vs. H data exhibits a clearly butterfly-shaped hysteresis effect above 1.9 K for **1** (Fig. S5).

Conclusions

We have synthesized a new mononuclear Dy(III)-complex of **1** which exhibits SIMs behavior. It has energy barrier 37.22 K over 9 K. Compared to its analogues of [Dy(dppz)(acac)₃]-CH₃OH, [Dy(dpq)(acac)₃] and [Dy(phen)(acac)₃], the different energy barrier observed in **1** might be resulted from the different coordination environment and ligand field around the Dy(III) ions resulted from the different auxiliary ligands. More importantly, these results might provide a useful approach for design and preparation of new SMMs.

Acknowledgments

We are grateful for financial support from National Nature Science Foundation of China (Nos. 21301109 and 21271120), Reward Fund for Outstanding Young and Middle Aged Scientists of Shandong Province (No. BS2012CL032), Jinan Science and Technology Bureau (OUT_06623) and "PCSIRT"

Notes and references

^a College of Chemistry, Chemical Engineering and Materials Science, Collaborative Innovation Center of Functionalized Probes for Chemical Imaging, Key Laboratory of Molecular and Nano Probes, Ministry of Education, Shandong Normal University, Jinan 250014, P. R. China. E-mail: yubindong@sdu.edu.cn

†Electronic Supplementary Information (ESI) available: The CIF and check CIF of **1**; Complex **1**, [Dy(dppz)(acac)₃]-CH₃OH, [Dy(dpq)(acac)₃] and [Dy(phen)(acac)₃] be seen from another angle; The Dy...Dy distances of **1**; The 1-D chain is assembled through π - π stacking interactions between aromatic ligand of **1**, PXRD pattern of complex **1**, Fitted broadness parameters α as a function of temperature for **1** and the magnetic hysteresis loop of **1** at 2 K. See DOI: 10.1039/b000000x/

‡CCDC 1007462 contains the supplementary crystallographic data for this paper. The data can be obtained free of charge from the Cambridge Crystallographic Data Centre via www.ccdc.cam.ac.uk/data_request/cif.

- E. Saitoh, H. Miyajima, T. Yamaoka, G. Tataru, *Nature*, 2004, **432**, 203.
- R. Sessoli, H. L. Tsai, A. R. Schake, S. Y. Wang, J. B. Vincent, K. Folting, D. Gatteschi, G. Christou, D. N. Hendrickson, *J. Am. Chem. Soc.*, 1993, **115**, 1804.
- D. Gatteschi, A. Caneschi, L. Pardi, R. Sessoli, *Science*, 1994, **265**, 1054.
- N. Roch, S. Florens, V. Bouchiat, W. Wernsdorfer, F. Balestro, *Nature*, 2008, **453**, 633.
- W. Wernsdorfer, R. Sessoli, *Science*, 1999, **284**, 133.
- D. N. Woodruff, R. E. P. Winpenny, R. A. Layfield, *Chem. Rev.* 2013, **113**, 5110.
- M. Cavallini, M. Facchini, C. Albonetti, F. Biscarini, *Phys. Chem. Chem. Phys.*, 2008, **10**, 784.
- M. N. Leuenberger, D. Loss, *Nature*, 2001, **410**, 789.
- C. Benelli, D. Gatteschi, *Chem. Rev.*, 2002, **102**, 2369.
- D. Aravena, E. Ruiz, *Inorg. Chem.* 2013, **52**, 13770.
- T. Glaser, *Chem. Commun.*, 2011, **47**, 116.
- A. Das, K. Gieb, Y. Krupskaya, S. Demeshko, S. Dechert, R. Klingeler, V. Kataev, B. Büchner, P. Müller, F. Meyer, *J. Am. Chem. Soc.*, 2011, **133**, 3433.
- Gao, F.; Cui, L.; Liu, W.; Hu, L.; Zhong, Y. W.; Li Y. Z.; Zuo, J. L. *Inorg. Chem.* 2013, **52**, 11164.
- P. D. W. Boyd, Q. Li, J. B. Vincent, K. Folting, H. R. Chang, W. E. Streib, J. C. Huffman, G. Christou, D. N. Hendrickson, *J. Am. Chem. Soc.*, 1988, **110**, 8537.
- R. Sessoli, D. Gatteschi, A. Caneschi, M. A. Novak, *Nature*, 1993, **365**, 141.
- L. J. Batchelor, I. Cimatti, R. Guillot, F. Tuna, W. Wernsdorfer, L. Ungur, L. F. Chibotaru, V. E. Campbell, T. Mallah, *Dalton Transactions*, DOI:10.1039/C4dt00846d.
- J. J. Le Roy, L. Ungur, I. Korobkov, L. F. Chibotaru, M. Murugesu, *J. Am. Chem. Soc.*, 2014, **136**, 8003.
- L. Ungur, J. J. Le Roy, I. Korobkov, M. Murugesu, L. F. Chibotaru, *Angew. Chem. Int. Ed.* 2014, **53**, 4413.
- A. Caneschi, D. Gatteschi, R. Sessoli, A. L. Barra, L. C. Brunel, M. Guillot, *J. Am. Chem. Soc.*, 1991, **113**, 5873.
- K. Katoh, R. Asano, A. Miura, Y. Horii, T. Morita, B. K. Breedlove, M. Yamashita, *Dalton Trans.*, 2014, **43**, 7716.
- J. L. Liu, W. Q. Lin, Y. C. Chen, J. D. Leng, F. S. Guo, M. L. Tong, *Inorg. Chem.*, 2013, **52**, 457.
- M. Gonidec, E. S. Davies, J. McMaster, D. B. Amabilino, J. Veciana, *J. Am. Chem. Soc.*, 2010, **132**, 1756.
- N. Ishikawa, M. Sugita, W. Wernsdorfer, *J. Am. Chem. Soc.*, 2005, **127**, 3650.
- G. Karotsis, S. Kennedy, S. J. Teat, C. M. Beavers, D. A. Fowler, J. J. Morales, M. Evangelisti, S. J. Dalgarno, E. K. Brechin, *J. Am. Chem. Soc.*, 2010, **132**, 12983.
- S. Osa, T. Kido, N. Matsumoto, N. Re, A. Pochaba, J. Mrozinski, *J. Am. Chem. Soc.*, 2004, **126**, 42.
- T. Kajiwara, M. Nakano, S. Takaishi, M. Yamashita, *Inorg. Chem.*, 2008, **47**, 8604.
- T. T. Cunha, J. Jung, M. E. Boulon, G. Campo, F. Pointillart, C. L. M. Pereira, B. L. Guennic, O. Cador, K. Bernot, F. Pineider, S. Golhen, L. Ouahab, *J. Am. Chem. Soc.*, 2013, **135**, 16332.
- P. H. Lin, T. J. Burchell, M. Murugesu, *Angew. Chem. Int. Ed.* 2008, **47**, 8848.
- X. L. Li, C. L. Chen, Y. L. Gao, C. M. Liu, X. L. Feng, Y. H. Gui, S. M. Fang, *Chem. Eur. J.*, 2012, **18**, 14632.
- P. H. Lin, T. J. Burchell, L. Ungur, L. F. Chibotaru, W. Wernsdorfer, M. Murugesu, *Angew. Chem. Int. Ed.*, 2009, **48**, 9489.
- R. J. Blagg, C. A. Muryn, E. J. L. McInnes, F. Tuna, R. E. P. Winpenny, *Angew. Chem.*, 2011, **123**, 6660.
- S. J. Liu, J. P. Zhao, W. C. Song, S. D. Han, Z. Y. Liu, X. H. Bu, *Inorg. Chem.*, 2013, **52**, 2103.
- F. S. Guo, J. L. Liu, J. D. Leng, Z. S. Meng, Z. J. Lin, M. L. Tong, S. Gao, L. Ungur, L. Chibotaru, *Chem. Eur. J.*, 2011, **17**, 2458.
- H. S. Ke, P. Gamez, L. Zhao, G. F. Xu, S. F. Xue, J. K. Tang, *Inorg. Chem.*, 2010, **49**, 7549.
- F. Gao, M. X. Yao, Y. Y. Li, Y. Z. Li, Y. Song, J. L. Zuo, *Inorg. Chem.*, 2013, **52**, 6407.
- H. S. Ke, G. F. Xu, Y. N. Guo, P. Gamez, C. M. Beavers, S. J. Teat, J. K. Tang, *Chem. Commun.*, 2010, **46**, 6057.
- Y. N. Guo, G. F. Xu, P. Gamez, L. Zhao, S. Y. Lin, R. P. Deng, J. K. Tang, H. J. Zhang, *J. Am. Chem. Soc.*, 2010, **132**, 8538.
- C. M. Liu, D. Q. Zhang, D. B. Zhu, *Inorg. Chem.* 2013, **52**, 8933.
- N. Ishikawa, M. Sugita, W. Wernsdorfer, *J. Am. Chem. Soc.*, 2005, **127**, 3650.
- S. O. Kido, T. N. Matsumoto, N. Re, A. Pochaba, J. Mrozinski, *J. Am. Chem. Soc.*, 2004, **126**, 420.
- E. K. Brechin, *Chem. Commun.*, 2005, 5141.
- G. F. Xu, P. Gamez, J. K. Tang, R. Clérac, Y. N. Guo, Y. Guo, *Inorg. Chem.*, 2012, **51**, 5693.
- J. D. Rinehart, J. R. Long, *Chem. Sci.*, 2011, **2**, 2078.
- H. Ke, L. Zhao, Y. Guo, J. Tang, *Inorg. Chem.*, 2012, **51**, 2699.
- Y. Song, F. Luo, M. Luo, Z. Liao, G. Sun, X. Tian, Y. Zhu, Z. Yuan, S. Liu, W. Xu, X. Feng, *Chem. Commun.*, 2012, **48**, 1006.
- N. Ishikawa, *Polyhedron*, 2007, **26**, 2147.
- S. Takamatsu, T. Ishikawa, S. Koshihara, N. Ishikawa, *Inorg. Chem.*, 2007, **46**, 7250.
- N. Ishikawa, Y. Mizuno, S. Takamatsu, T. Ishikawa, S. Koshihara, *Inorg. Chem.*, 2008, **47**, 10217.
- N. Ishikawa, S. Otsuka, Y. Kaizu, *Angew. Chem. Int. Ed.*, 2005, **44**, 731.
- S. Sakaue, A. Fuyuhiko, T. Fukuda, N. Ishikawa, *Chem. Commun.*, 2012, **48**, 5337.
- K. Katoh, T. Kajiwara, M. Nakano, Y. Nakazawa, W. Wernsdorfer, N. Ishikawa, B. K. Breedlove, M. Yamashita, *Chem. Eur. J.*, 2011, **17**, 1117.
- N. Ishikawa, M. Sugita, T. Ishikawa, S. Koshihara, Y. Kaizu, *J. Phys. Chem. B.*, 2004, **108**, 11265.
- N. Ishikawa, M. Sugita, T. Ishikawa, S. Koshihara, Y. Kaizu, *J. Am. Chem. Soc.*, 2003, **125**, 8694.

54. N. Ishikawa, M. Sugita, W. Wernsdorfer, *Angew. Chem.*, 2005, **117**, 2991.
55. N. Ishikawa, Y. Mizuno, S. Takamatsu, T. Ishikawa, S. Koshihara, *Inorg. Chem.*, 2008, **47**, 10217.
56. S. D. Jiang, B. W. Wang, G. Su, Z. M. Wang, S. Gao, *Angew. Chem. Int. Ed.*, 2010, **49**, 7448.
57. Y. Bi, Y. N. Guo, L. Zhao, Y. Guo, S. Y. Lin, S. D. Jiang, J. Tang, B. W. Wang, S. Gao, *Chem. Eur. J.*, 2011, **17**, 12476.
58. G. J. Chen, Y. N. Guo, J. L. Tian, J. Tang, W. Gu, X. Liu, S. P. Yan, P. Cheng, D. Z. Liao, *Chem. Eur. J.*, 2012, **18**, 2484.
59. G. J. Chen, C. Y. Gao, J. L. Tian, J. Tang, W. Gu, X. Liu, S. P. Yan, D. Z. Liao, P. Cheng, *Dalton Trans.*, 2011, **40**, 5579.
60. D. P. Li, T. W. Wang, C. H. Li, D. S. Liu, Y. Z. Li.; X. Z. You, *Chem. Commun.*, 2010, **46**, 2929.
61. D. P. Li, X. P. Zhang, T. W. Wang, B. B. Ma, C. H. Li, Y. Z. Li, X. Z. You, *Chem. Commun.*, 2011, **47**, 6867.
62. X. L. Mei, Y. Ma, L. C. Li, D. Z. Liao, *Dalton Trans.*, 2012, **41**, 505.
63. M. Jeletic, P. H. Lin, J. J. L. Roy, I. Korobkov, S. I. Gorelsky, M. Murugesu, *J. Am. Chem. Soc.* 2011, **133**, 19286.
64. S. D. Jiang, S. S. Liu, L. N. Zhou, B. W. Wang, Z. M. Wang, S. Gao, *Inorg. Chem.*, 2012, **51**, 3079.
65. D. N. Woodruff, F. Tuna, M. Bodensteiner, R.E. P. Winpenny, R. A. Layfield, *Organometallics*, 2013, **32**, 1224.
66. L. Sorace, C. Benellib, D. Gatteschi, *Chem. Soc. Rev.*, 2011, **40**, 3092.
67. Sheldrick GM. SHELXS 97, Program for the Solution of Crystal Structures, University of Göttingen, Germany, 1997.
68. Sheldrick GM. SHELXL 97, Program for the Refinement of Crystal Structures, University of Göttingen: Germany, 1997.
69. Y. Ma, G. F. Xu, X. Yang, L.C. Li, J. K. Tang, S. P. Yan, P. Cheng, D.Z. Liao, *Chem. Commun.*, 2010, **46**, 8264.
70. B. Bleaney, *J. Magn. Reson.*, 1972, **8**, 91.
71. Y. Wang, X. L. Li, T. W. Wang, Y. Song, X. Z. You, *Inorg. Chem.*, 2010, **49**, 969.
72. S. M. Aubin, Z. Sun, L. Pardi, J. Krzystek, K. Folting, L. C. Brunel, A. L. Rheingold, G. Christou, D. N. Hendrickson, *Inorg. Chem.*, 1999, **38**, 5329.
73. K. S. Cole, R. H. Cole, *J. Chem. Phys.*, 1941, **9**, 341.
74. M. X. Yao, Q. Zheng, K. Qian, Y. Song, S. Gao, J. L. Zuo, *Chem. Eur. J.*, 2013, **19**, 294.
75. W. E. Buschmann, J. Ensling, P. Gu, J. S. Miller, *Chem. Eur. J.*, 1999, **5**, 3019.

45